Enhanced dynamic interpretation from correlating well activity to frequently acquired 4D seismic signatures

Yi Huang and Colin MacBeth, Heriot-Watt University
Olav Barkved and Jean-Paul van Gestel, BP
Ole Petter Dybvik, Statoil

Quantitative 4D seismic interpretation can be successfully achieved by exploiting the causal link between the temporal variation in well activity and the 4D seismic signatures they induce. This is achieved by capturing in mathematical form the common interpretational practice of identifying the origin of dynamic signals in the 4D seismic volumes or maps on the basis of their association with a particular injector or producer. Thus, for example, a region of reservoir hardening (impedance increase) around a producer may be interpreted as a signal of pressure decrease. Similarly, an area of softening (impedance decrease) around an injector is interpreted as a signal of pressure increase when pressures are above bubble point. In the literature, a hardwired integration between the seismic and engineering domain has been obtained to some extent using methods such as seismic history matching, where the observed seismic and well production history data are simultaneously fit by predictions from a common simulation model. However, this approach is computationally expensive and suffers from nonuniquenesses, inaccuracies in the petroelastic model, and is ultimately only as accurate as the model itself. As an alternate approach, we reconcile here the well production history and time-lapse seismic data in the data domain without the need for a model. This approach involves the use of many frequently repeated seismic surveys shot over the same field, and mathematically correlates changes in the mapped seismic attributes directly to the fluid volumes injected and produced from the wells. Thus, well data normally used exclusively for history matching in the reservoir engineering domain can now also be directly integrated with the time-lapse seismic data.

The technique highlighted here is appropriate as in recent times many marine 4D seismic data sets have already been shot and there are indeed many repeats over the same field (for example, Sandø et al., 2009). Furthermore, the growing popularity of reservoir monitoring using permanent reservoir installations has opened up the possibility of acquiring highly repeatable seismic surveys frequently. Examples are the Life of Field Seismic (LoFS) projects on the Valhall Field (Barkved et al., 2006) which have so far delivered over 12 3D seismic surveys shot 2–10 months apart. Similar projects have been implemented on Clair Field, Snorre Field, Ekofisk Field, Jubarte Field (Brazil), and Azeri-Chirag-Gunashli Field (Azerbaijan) (2011 EAGE workshop on Permanent Reservoir Monitoring Using Seismic Data). In the wider context, many fields such as Norne (Osdal et al., 2006) and Schiehallion (Floricich et al. 2008) have been repeatedly shot with seven or eight towed-streamer surveys at intervals of 12–24 months apart. It is already known that frequent repeats can be beneficial when filtering out undesirable noise such as water-bottom multiples or when overlapping coherency signals for identifying compartmentalization (Stammeijer and Hatchell, 2011). Thus, the technique described here has benefits to an ever increasing range of fields. It will be shown that by establishing a correlation with the production data over survey periods, the dynamic connectivity of the reservoir can be imaged. The approach is illustrated by application to three separate time-lapse marine seismic data sets.

Linking well activity to the 4D seismic response

The theory below describes how the produced and injected volumes can be linked to a 4D seismic attribute. At any particular location in the reservoir, the 4D signature is a direct function of the production and injection history of wells connected to that location. Consider, as an example, a pressure-dominated 4D seismic attribute. By modifying the proposed pressure-saturation equation of MacBeth et al. (2006) to involve only well volumes, the 4D signature evaluated between a specific time period is seen to be related to the cumulative sum of the produced or injected volumes from these group of wells (Huang and MacBeth, 2009). For many seismic surveys shot over the same location (x,y) at different intervals T_k (where k=1,P) of calendar time, it is now possible to form a

Figure 1. *Location of the three fields used in this work. Schiehallion is west of the Shetland Isles; Valhall is in the southernmost corner of the Norwegian continental shelf; and Norne is in the Norwegian Sea.*

time sequence of mapped 4D signatures ΔA_k associated with a corresponding sequence of cumulative volumes ΔV_{jk} from the measured data from M producers and N injectors

$$\Delta A_k(x,y) = G\left[\sum_{i=1}^{M} B_o \Delta V_{ik}^{o} + \sum_{j=1}^{M} B_w \Delta V_{jk}^{w} + \sum_{l=1}^{N} B_w \Delta V_{lk}^{w}\right] \quad (1)$$

where the lumped term G on the right contains information about the geology, fluid properties, petroelastic model, connectivity, and degree of compartmentalization (and hence reservoir boundary conditions). B_o and B_w are the formation volume factors for oil and water, respectively, ΔV^o the oil volume difference, and ΔV^w the produced or injected water-volume difference. It appears that the 4D signature can be linearly correlated to the cumulative well volumes when observed as a sequence of many different elapsed times. Flow simulation and seismic modeling studies have validated this relation for different seismic attributes and reservoirs (Huang and MacBeth, 2011; Huang et al., 2011).

With multiple seismic surveys available, a time sequence can be created by making difference maps for all possible pairs of surveys (i.e., $A(x,y)$ for all T_k). In particular, for n surveys, there are $n(n-1)/2$ combinations of differences. It is the concatenation of these different combinations that forms the sequences used in this method. For example, for ten repeated surveys, a sequence with 45 distinct difference maps can be generated. The seismic attribute sequence $(\Delta V_1, \Delta V_2, \Delta V_3, ..., \Delta V_{45})$ for each seismic bin location (x,y) is linked to the corresponding sequence of cumulative volumes for a connected well group by calculating the normalized cross-correlation (*NCC*) statistic (Bevington, 1975). A high correlation implies a connection to the particular well or well group via Equation 1. This measure is calculated for each seismic bin location (x,y), thereby producing a map of NCC across the reservoir region of interest. When mapped, this seismic-to-well correlation measure maintains the lateral resolution of the seismic and is therefore usually higher than that of the flow simulation model.

Adding more repeat surveys or alternations in well rate lead to an increasingly complicated and finer-scale time sequence, hence increasing the statistical robustness of the normalized cross-correlation measure. To ensure stability, a minimum credibility threshold is needed for the NCC maps, as for a particular size of time sequence the cross-correlation coefficient is only statistically significant above a certain coefficient value. Below this threshold, there is a chance that samples drawn at random can yield the same coefficient (Bevington, 1975). For example, for 45 points, sequences with correlation coefficients greater than 0.38 are significant with a 99% confidence, whereas for 10 points this threshold becomes 0.77. Another reason for thresholding the NCC maps shown in the field examples is to focus on the 4D signature induced only by a particular well or group of wells, and to exclude the contributions from other wells. The correlation coefficient between the members of the selected well group of interest and the seismic sequence must in this case be higher than the sequence correlation between the excluded wells and the selected group. Thus, the final threshold used in a particular work is based on the quality of the seismic data and main objectives of the analysis. Whilst the explanation above relates only to the development of pressure, it has been found by practical application that the method may also be successfully applied to reservoirs in which saturation and pressure signals control the 4D seismic, or the case of the pressure signal being enhanced by compaction effects.

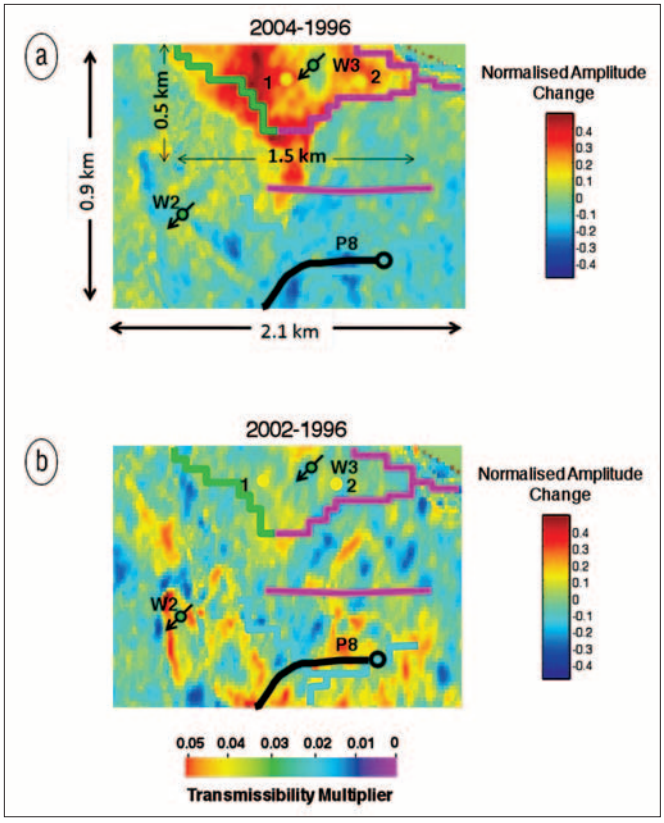

Figure 2. *Two 4D seismic signatures selected from the sequence of available data for Schiehallion, with transmissibility barriers from the simulator superimposed for reference: (a) signature for 04–96 and (b) signature for 02–96.*

Applications to observed data

The technique proposed in this work has been applied to data sets from three North Sea fields: Schiehallion, Valhall, and Norne (Figure 1). Each example demonstrates different reservoir challenges and connectivity issues.

Schiehallion Field. This field consists of several layers of turbidite channel sands of Tertiary age, with total thickness of 10–50 m and lying at approximately 2000 m subsea (Leach et al. 1999). The reservoir quality is good (28% porosity and 600 mD permeability); however, production is challenging due to compartmentalization. The relationship between structural/depositional complexities and various producer-injector communication scenarios is well documented in the literature for this field (Parr and Marsh, 2000). Thus, the main focus of development and production is knowledge of the reservoir connectivity, and this has been addressed to some degree using 4D seismic. Past studies have found fine-scale details, subtle barriers and, more recently, connected geobodies (Martin and MacDonald, 2010) with which to effectively update the flow

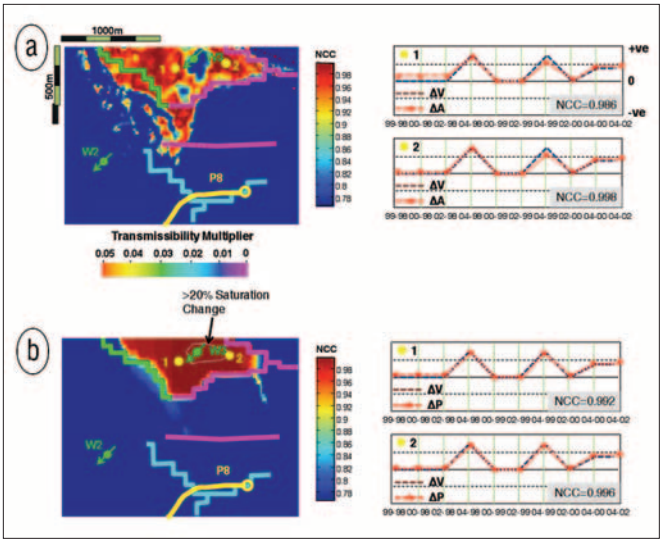

Figure 3. *Schiehallion Field results. (right) Correlation panels for two specific locations (marked as filled circles 1 and 2 on the maps) around injector W3, comparing cumulative fluid volume changes ΔV (black dashed lines) and the corresponding 4D signatures ΔA (red dashed lines). (left) Maps of the normalized cross-correlation attribute thresholded at a 99% confidence level: (a) results for observed 4D signatures and (b) results for the corresponding pressure change from the simulator, with outline of saturation changes > 20% drawn. Colored lines are transmissibility barriers extracted from the simulator (barriers in both the x and y directions are combined).*

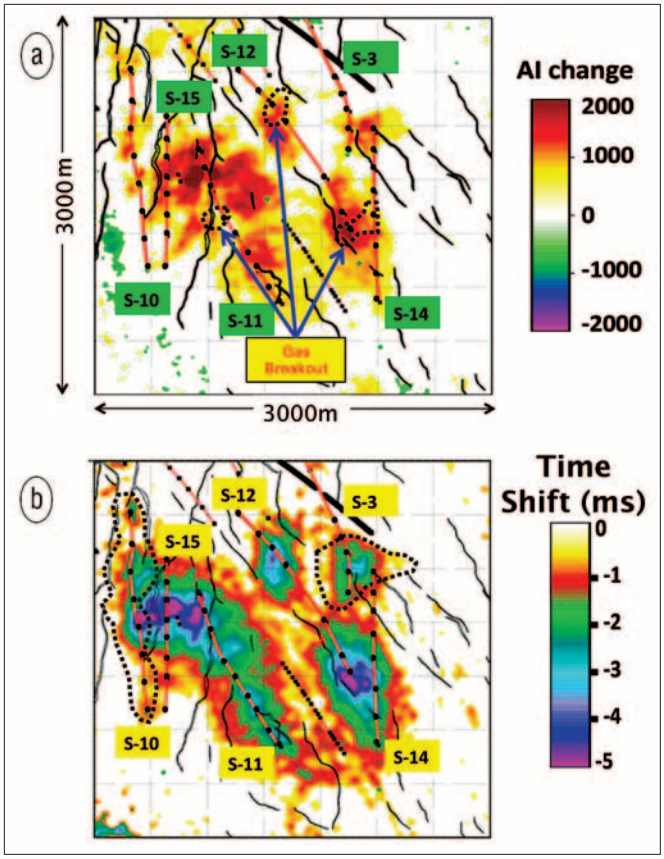

Figure 4. *The well paths and perforation locations for the major production wells on the south flank of Valhall overlaid on (a) mapped AI change between LoFS10 and the baseline survey and (b) time-shift attribute. The positive AI change and negative time shift indicate the reservoir hardening caused by strong reservoir compaction due to pressure depletion in the reservoir. The dotted circular areas in (a) correspond to the zones of gas evolution identified by the correlation technique in this paper; in (b), they indicate the regions controlled by the Group 2 wells identified by our method.*

simulation model. With multiple seismic surveys acquired over a common field-wide area, there is an opportunity to resolve well interpretation ambiguities using the proposed method. For our work, we use data from 1996 (preproduction baseline), 1999, 2000, 2002, and 2004. For each survey, rms-mapped amplitude is evaluated for an interval between the picked top and base of the T31 reservoir.

The five repeated seismic surveys generate in total ten mapped 4D signatures, and these are arranged as a time sequence for each spatial location and the NCC obtained. Figure 2 shows the injector W3 in the central north portion of Segment 4. On the sector scale, it was intended to supply pressure to P8 in the south and P9 in the east (outside the figure perimeter). However, W3 was found to have injected into an unseen small isolated triangular fault block of roughly 1 × 0.5 km, bounded along its northern edge by a major east-west sealing fault, and along its remaining edges by smaller faults or stratigraphic barriers. The 4D seismic response shows a strong softening signal (Figure 2a) due to pressure increase (pressure change of 2000 psi or 13.8 MPa) relative to before injection (Figure 2b). Transmissibility multipliers assigned to the simulation model along the block edges suggest that a small amount of leakage to the west is anticipated. Conventional 4D seismic interpretation does not clearly resolve the leakage due to presence of a similar magnitude of 4D changes beyond the edge of this compartment towards other wells (W2 and P9). Figure 3a shows the time sequence of cumulative changes in fluid volume alongside the seismic rms amplitude changes for two reference locations inside the fault block. This validates the strong linear correlation between the pressure change spread across the entire fault block and the change in cumulative fluid volumes at well W3. The mapped normalized cross-correlations (NCC) are high and the fault block is readily delineated by this attribute. Most importantly, a scattered distribution of high correlation coefficients is observed beyond but immediately close to the western barriers, clearly indicating a lack of seal. This observation is consistent with the mapped NCC attribute calculated from the predicted pressure changes derived from the simulator (shown for visual comparison only in Figure 3b). The NCC results help clarify the dynamic nature of the flow barriers by removing irrelevant signals uncorrelated to the well activity.

Valhall Field. The Valhall Field is a well-known high-porosity, low-permeability chalk reservoir with production activity directly affected by the rock compaction and active geomechanical effects (Barkved et al., 2003). Across the field, the seismic response is strongly related to the pressure reduction and the resulting physical compaction process. Along each horizontal well path, the 4D response is found to be closely associated with individual perforations and their performance. Barkved et al. (2009) demonstrated use of such

		Group 1				Group 2	
		S-11	S-12	S-14	S-15	S-3	S-10
Group 1	S-11	1					
	S-12	0.988	1				
	S-14	0.991	0.983	1			
	S-15	0.971	0.983	0.982	1		
Group 2	S-3	0.516	0.573	0.833	0.448	1	
	S-10	0.516	0.573	0.76	0.448	0.943	1

Table 1. *Normalized correlation coefficients calculated for cumulative volume time sequences from the south flank of Valhall Field.*

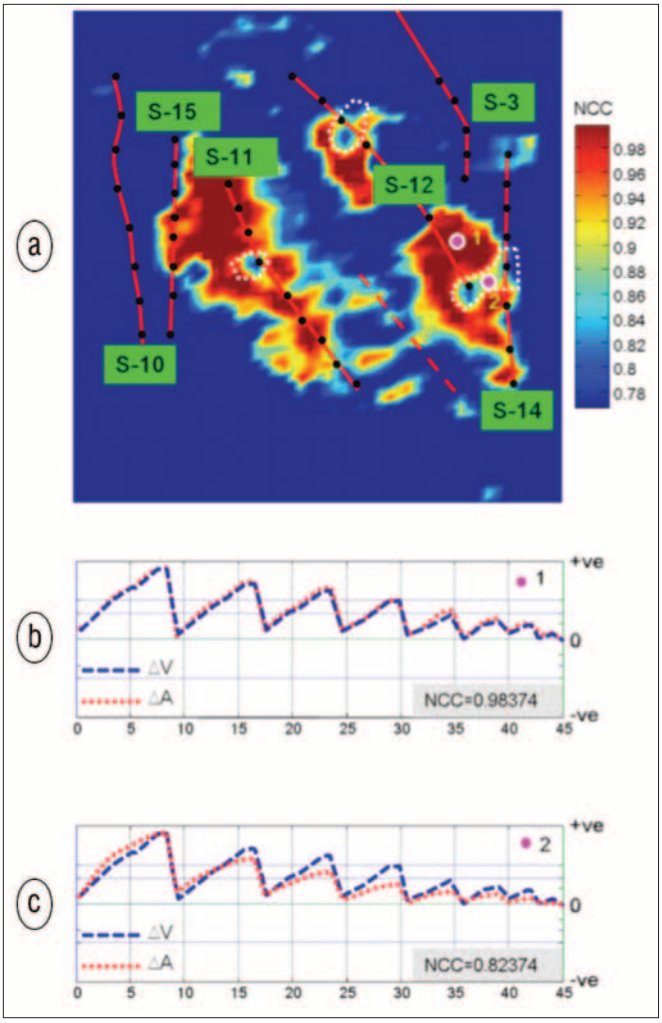

Figure 5. *(a) NCC map computed using the well sequence of S-12 from Valhall. Low correlation regions are observed and highlighted using dashed lines. The time sequences of seismic change ΔA and cumulative volume ΔV are computed for two observation points, 1 and 2, where the 4D seismic changes are dominated by (b) reservoir compaction, and (c) a combination of reservoir compaction and the effect of gas breakout.*

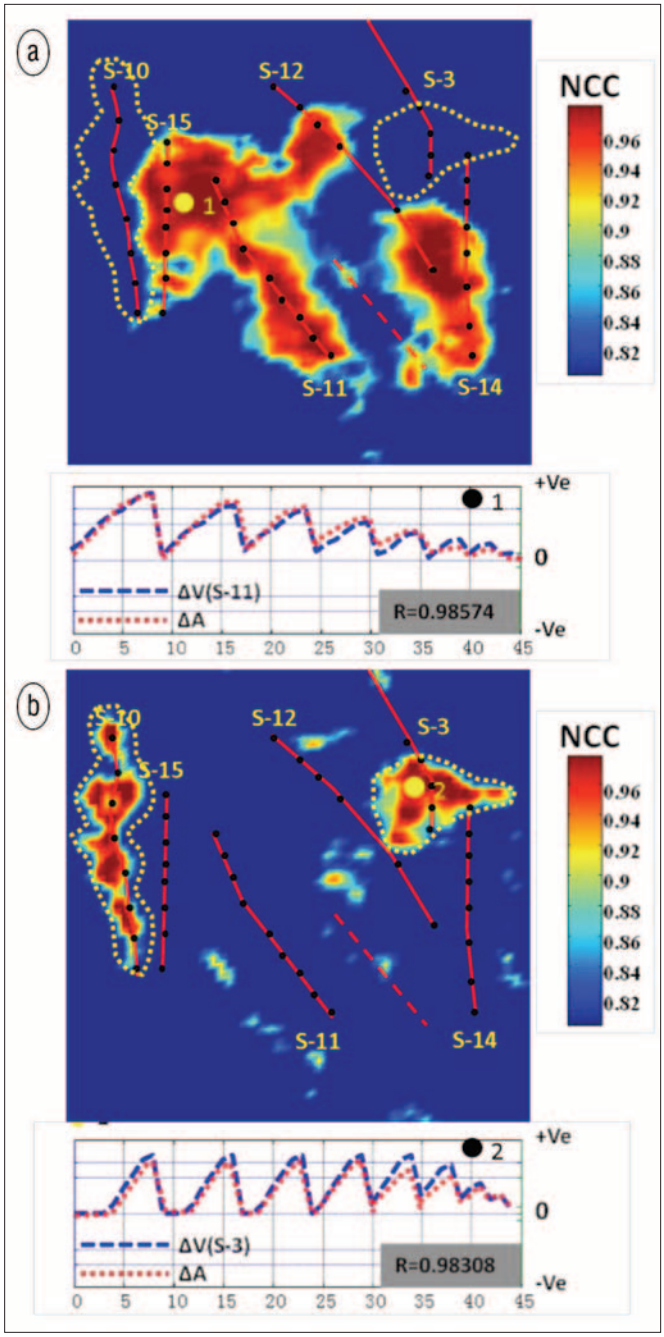

Figure 6. *Valhall results. Normalized cross-correlation (NCC) maps based on time-shift attribute for the two groups of wells: (a) Group 1 = S-10 and S-3 and (b) Group 2 = S-11, S-12, S-14, and S-15 on the south flank of Valhall. There is a strong correlation between the 4D seismic (ΔA) and the well activity (ΔV).*

a production-to-seismic association by defining a "seismic PLT". Thus, information about the flow contribution from each perforation obtained previously from well-based PLTs can be extracted instead from the seismic. This is critical as it allows production engineers the opportunity to identify and critically analyse factors which affect perforation performance such as casing, rock formation, effective stress, and the gun system. The effective use of 4D seismic for interpretation is, however, restricted by a number of practical issues. For instance, long-reach horizontal producers and injectors are densely positioned, causing difficulties in isolating the individual well contributions. Also, gas coming out of solution due to pressure decrease below bubble point can mask the strong compaction response observed in the seismic data.

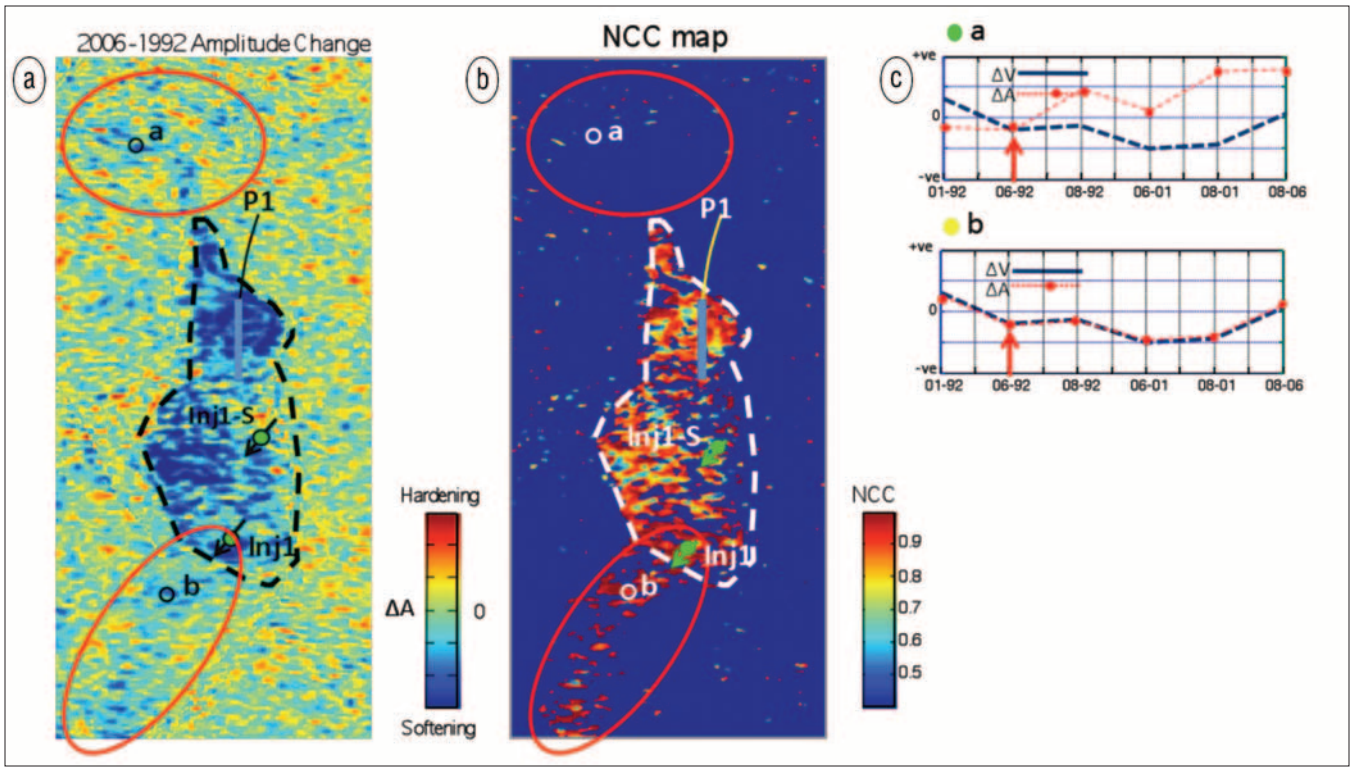

Figure 7. *Norne Field results. (a) Mapped amplitude difference between 2006 and 1992 over the G segment of Norne Field. (b) NCC map calculated over the same area based on total compartment volumes (net volumes of all the wells in G segment). (c) Correlation panels for two reference locations a and b, randomly selected in the two uncertain areas thought to be connected to G segment. The G segment is outlined in black and white dotted lines in (a) and (b), respectively.*

To confront these challenges, our technique is applied to the frequently acquired LoFS data. For this work, the baseline survey shot in the autumn of 2003 is available, together with ten repeat surveys shot at intervals of 3–6 months. From these data, a time series of 45 difference maps can be generated, and this represents an ideal data set for the well-correlation approach.

Figures 4a and 4b show the general development of positive changes in acoustic impedance (AI) and a negative time shift across the south flank of the field, respectively indicating a reservoir-hardening effect related to pressure reduction and the resulting compaction. It is also known that, at some of the well perforations, gas comes out of solution due to localized pore-pressure decline below bubble point, causing a reduction in impedance. The exact position of these regions is difficult to detect in the AI attribute due to the masking effect of compaction and interwell interference. To tackle this problem, the wells in this area influencing the seismic response are firstly divided into two groups according to their distinctive well activity, putting wells S-11, S-12, S-14, and S-15 in Group 1, and S-3 and S-10 in Group 2. Table 1 indicates the well-to-well correlation which shows the larger difference between the inter- and intrawell correlations. Figure 5 shows the resultant seismic-to-well correlation NCC map thresholded at 0.75, generated by correlating the AI signatures with S-12 (characterizing Group 1). The maps reveal two strong zones of correlation related to wells S-11 and S-12 and a weaker zone related to S-14, but also small circular regions of reduced correlation that are positioned over the well perforations. This correlation weakening is attributed to the exsolved gas disrupting and reversing the systematic hardening trend established between pressure depletion and the AI attribute. These zones are not evident at all in the maps of AI change in Figure 4a; however, a separate study (Barkved et al., 2009) has shown that complex multiple attributes can be designed to specifically illuminate gas zones at identical locations. These zones correspond to particularly active and competent perforations, with good connection to the formation, high reservoir quality and, hence, well developed pressure depletion. Similarly, Figures 6a and 6b show NCC results based on the time-shift attribute for Group 1 and 2 wells, respectively. In these maps, the boundary of the areas influenced by two closely spaced wells (S-10 and S-15) can be identified precisely. Interestingly, the 4D response as outlined in the polygon around S-3 was previously considered as a joint effect of S-3 and S-14 activity. However, the NCC maps calculated for both groups of wells suggest this 4D response is related only to S-3. The NCC results have thus helped to identify gas and resolve separate well responses.

Norne Field, Norwegian Sea. The Norne Field is a horst block consisting of several layers of Jurassic sequences. The reservoir rock is of very good quality with porosities of 25–32% and permeabilities of 200–2000mD (Osdal et al., 2006). For this particular study, the four surveys shot in 1992 (baseline), 2001, 2006, and 2008 are adopted for generation of sequences of seismic signatures as they exhibit mainly ex-

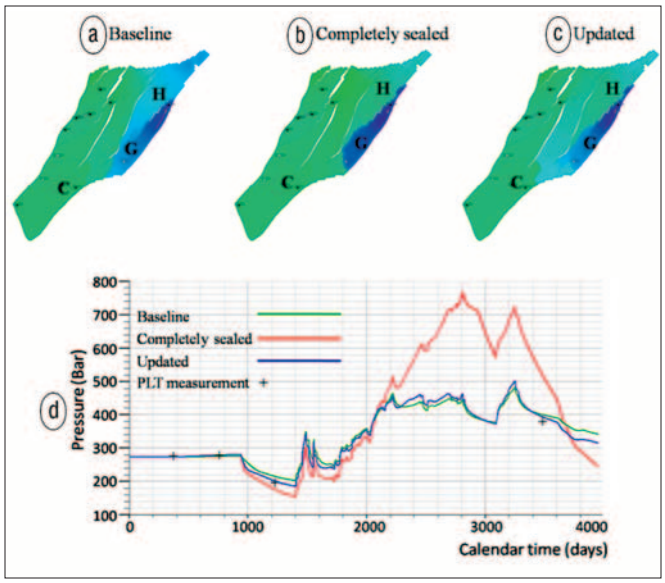

Figure 8. *Simulated pressure distribution in 2006 for Norne Field. (a) Baseline model used in this study. (b) Intermediate model showing the effect of a completely sealed G segment. (c) Updated model with the lower part of G segment open to C segment. (d) Simulated downhole pressure from updated model (blue line) exhibits better matching to the measured reservoir pressure from the sparsely measured PLT data compared to that from baseline and intermediate model (indicated by green and red lines, respectively).*

tensive pressure-driven signals across the segment. Our work focuses on the G segment of the field as it is considered to be relatively simple in terms of reservoir conditions; there is no initial gas, and oil is contained only in the uppermost Not Formation (25–30 m). It is believed that the G segment has little pressure communication with the rest of the reservoir and aquifer encroachment is not significant. Thus, we expect to see fluid volumes injected into or produced from the segment causing a corresponding change in the average pressure across the segment and resulting in a 4D seismic response. Figure 7a shows the 4D amplitude difference between 2006 and 1992, which is interpreted to be caused by increased reservoir pressure due to injected fluid volumes exceeding those produced. It is observed both on this 4D signature and those from other survey periods that the pressure change tends to occur uniformly in the G segment.

Two channel-like areas connected to the G segment are illuminated by a similar "softening" response, but the interpretation of these signals is unambiguous. Preliminary inspection offers two possible scenarios that can explain these signals: (1) these areas are pressurized by underlying connections to wells in the G segment, suggesting the segment is not completely closed as previously thought, or (2) that they are responses of production-induced effects in the neighboring segments, for example gas out of solution due to production in the upper area (Stær Field) and water injection in the lower area (possibly connected to the C segment). The NCC map from the well-to-seismic correlation technique shows mainly high correlations (Figures 7b and 7c). For the two proposed connections, however, only the lower one remains illuminated using NCC while the upper one is not—suggesting the latter is not in fact a connection. Based on the NCC result, the simulation model is updated in order to validate the interpretation (Figure 8). Figure 8d shows the simulated downhole pressure from the updated model in which the finger-like connection to the lower portion of the segment is now incorporated (Figure 8c). For the model shown in Figures 8a and 8b, a general 2.0–2.5 MPa difference is found between the predicted pressure from the model and measured pressure from the available PLT data. This mismatch appears to be reduced for the updated model. Thus, it is concluded that this model-updating is engineering evidence that lends support to our interpretation based on the NCC map.

Discussion and conclusions

In this article, it has been demonstrated that it is possible to correlate mapped 4D seismic signatures from multiply acquired repeat surveys with the cumulative volumes produced at wells over these time periods. This means that well data used predominantly for history matching in the reservoir engineering domain can also be used to constrain the observed 4D seismic data. This makes the reservoir signal extracted from the seismic more robust and informative. Using this approach, areas can be identified that are strongly consistent with the well activity and, hence, directly connected to the wells. Several examples are shown where this unique benefit resolves the ambiguities in dynamic interpretation without the use of a reservoir or petroelastic models. For example, the results from the Valhall study reveal clear boundaries between regions influenced by closely positioned interfering wells. In the Schiehallion and Norne examples, the approach helps to improve our knowledge of reservoir connectivity by highlighting regions associated with the compartment being studied, and can thus be used to update the simulation model.

It is found that the effectiveness of the proposed technique improves with the number and frequency of 4D surveys and an increased complexity of well activity. The minimum number of surveys required for the technique to be valid is four (i.e., one baseline plus three monitor surveys), and with less repeats than that a meaningful correlation cannot be constructed. The Valhall Field with more than ten highly repeatable surveys represents the ideal data to test the technique. It is therefore expected that the applicability of the technique will be broadened not only as permanent reservoir monitoring (PRM) becomes more popular but also as the number of high-definition towed-streamer surveys increases across most fields in the future. TLE

References

Barkved, O. I., A. G. Bærheim, D. J. Howe, J. H. Kommedal, and F. Nicol, 2003, Life of Field seismic implementation—"First at Valhall": 65th Conference and Exhibition, EAGE, Extended Abstracts.

Barkved, O. I., J. P. Van Gestel, L. S. Bergsvik, I. Stockden, and J. H. Kommedal, 2009, Seismic PLT—linking seismic time-lapse responses to production and injection data: 65th Conference and Exhibition, EAGE, Extended Abstracts, R033.

Bevington, B. R., 1975, Data reduction and error analysis for the physical sciences: McGraw-Hill.

Huang, Y. and C. MacBeth, 2009, Direct correlation of 4D seismic and well activity for dynamic reservoir interpretation: 79th Annual International Meeting, SEG, Expanded Abstracts, 3840–3844.

Huang, Y., C. MacBeth, O. Barkved, and J.-P. van Gestel, 2011, Correlation of well activity to time-lapsed signatures in the Valhall Field for enhanced dynamic interpretation: First Break, **29**, 37–44.

Huang, Y. and C. MacBeth, in press, Direct correlation of 4D seismic and well activity for a clarified dynamic reservoir interpretation: Geophysical Prospecting.

Floricich, M., A. Evans, D. McCormick, G. Jenkins, and J. Stammeijer, 2008, Adding the temporal coherence dimension to 4D seismic data—assessing connectivity in the Schiehallion Field: 65th Conference and Exhibition, EAGE, Extended Abstracts, E017.

Leach, H. M., N. Herbert, A. Los, and R. L. Smith, 1999, The Schiehallion development: Petroleum Geology Conference series, **5**, 683–692.

MacBeth, C., M. Floricich, and J. Soldo, 2006, Going quantitative with 4D seismic analysis: Geophysical Prospecting, **54**, no. 3, 303–317, doi:10.1111/j.1365-2478.2006.00536.x.

Martin, K. and C. MacDonald, 2010, The Schiehallion Field: Applying a geobody modeling approach to piece together a complex turbidite reservoir: Devex 2010, O.33

Osdal, B., O. Husby, H. Aronsen, N. Chen, and T. Alsos, 2006, Mapping the fluid front and pressure buildup using 4D data on Norne Field: The Leading Edge, **9**, no. 9, 1134–1141, doi:10.1190/1.2349818.

Parr R. S. and M. Marsh, 2000, Development of 4-D reservoir management West of Shetland: World Oil, September, 39–47.

Sandø, I., O.-P. N. Munkvold, and R.M. Elde, 2009, Two decades of 3D geophysical developments—experiences, value creation, and future trends. World Oil, 230, (10).

Stammeijer, J. and P. Hatchell, 2011, Opportunities and challenges from bringing PRM to the field: EAGE Workshop on Permanent Reservoir Monitoring, Abstract 10389.

Acknowledgments: We thank BP and Schiehallion Field partners (BP, Shell, Amerada Hess, Statoil, Murphy Oil, and OMV); BP Norge and the Valhall partnership (BP Norge AS, Amerada Hess Norge, Total E&P, Norge AS, and A/S Norske Shell); and Statoil and the Norne Field partners (Statoil, Petoro, ENI) for permission to publish this description. We thank sponsors of the Edinburgh Time Lapse Project, Phase III and IV (BG, BP, Chevron, ConocoPhillips, EnCana, ENI, ExxonMobil, Hess, Ikon Science, Landmark, Maersk, Marathon, Norsar, Ohm, Petrobras, Shell, Statoil, Total, and Woodside) for supporting our research. We thank Schlumberger for the use of their Petrel and Eclipse software.

Corresponding author: colin.macbeth@pet.hw.ac.uk